The Venusian atmospheric oxygen ion escape: Extrapolation to the early Solar System

M. Persson[1,2], Y. Futaana[1], R. Ramstad[3], K. Masunaga[3], H. Nilsson[1], M. Hamrin[2], A. Fedorov[4], and S. Barabash[1]

[1]Swedish Institute for Space Physics, Kiruna, Sweden.

[2]Department of Physics, Umeå University, Umeå, Sweden.

[3]Laboratory for Atmospheric and Space Physics, University of Colorado Boulder, Boulder, Colorado, USA

[4]IRAP, CNRS, Toulouse, France.

Key Points:

- **1 The current escape of O^+ from Venus is energy-limited, not source-limited**
- **2 The extrapolated mass loss through ion escape account for 6 mbar of the current Venusian atmosphere**
- **3 The total mass loss from ion escape cannot account for the loss of a large water inventory at Venus**

Abstract

We investigate the escape rates of O^+ through the magnetotail of Venus and its dependence on the upstream solar and solar wind conditions, using Venus Express measurements. We find that the O^+ escape rate increases with the solar wind energy flux as $Q_{O+} = Q_0 \cdot F_{energy,SW}^{0.5\pm0.3}$, where $Q_0 = 7.1 \cdot 10^{16}$ for high EUV and $Q_0 = 8.5 \cdot 10^{16}$ for low EUV. As the solar EUV flux did not increase significantly over the studied solar cycle, the variation of the escape rates with the solar EUV flux is not strong in this dataset. Nevertheless, the escape rate decreases with higher EUV as there is an increase in the Venusward fluxes. From the relation between the escape rate and the solar wind energy flux we extrapolated the escape rates to 3.9 Ga. The results indicate a total loss of $3.6 \cdot 10^{16}$ kg of water through non-thermal ion escape, or equal to ~0.3 m of a global equivalent layer of water, and therefore cannot account for the loss of an historical terrestrial-like ocean (~10^{21} kg) in the Venusian atmosphere.

Plain Language Summary

Today, Venus has a dry atmosphere, but some measurements indicate that in its early history Venus had a terrestrial-like ocean. In this study, we investigate how much of this water may have escaped through non-thermal ion escape over the past 3.9 Gyrs of the Venusian history. Using the present relation between the O^+ escape rates and the upstream solar wind energy flux, we find that the atmosphere presumably has lost ~0.3 m of water, if spread evenly over the entire surface, from the atmosphere. This is orders of magnitude lower than the presumed terrestrial-like ocean that was present in the Venusian early history. This indicates that either the Venusian atmosphere did not have as much water in its atmosphere as previously assumed, or that some other mechanisms have acted to efficiently remove the water from the atmosphere.

1. Introduction

Today, the Venusian atmosphere is thick, dry, and has a high CO_2 content, but it was likely different in its early history. Observations of the deuterium-to-hydrogen ratio and surface properties indicate that Venus had large amounts of water in its atmosphere billions of years ago (Donahue et al., 1997; Ingersoll, 1969; Taylor et al., 2018, and references therein). The high deuterium-to-hydrogen ratio indicate a fractionated long-term escape, where for example the lighter hydrogen escape easier than the heavier deuterium (Donahue et al., 1997). On the other hand, the observed high ratio may partly be explained by a catastrophic resurfacing event and accompanied outgassing within the past 1 billion years, or an extremely large comet impact (Taylor and Grinspoon, 2009). Distinguishing between these different interpretations is important for characterizing the evolution of the Venusian atmosphere. Therefore, it is important to determine the escape to space, how it affects the different species, particularly hydrogen and oxygen that composes water, and how it has evolved over time.

Billions of years ago, the solar extreme ultraviolet radiation (EUV) fluxes was 100-1000 times stronger than it is today (Ribas et al., 2005). The strong EUV flux would have significantly heated the atmosphere, expanded it, and caused a hydrodynamic escape of hydrogen to space, which by drag forces would have led to the escape of neutral oxygen (Gillmann & Tackley, 2014). Today, the thermal and hydrodynamical escape of neutral atoms to space is negligible, as the upper atmosphere of Venus is cooled by the CO_2 emissions in the upper atmosphere (Woodsworth and Pierrehumbert, 2013). Instead, the escape of neutral atoms comes mainly from the non-thermal escape through photochemical reactions and sputtering. The escape from photochemical reactions is only important for hydrogen, not O, due to the high escape energy for O (McElroy et al., 1982). Escape due to sputtering of neutral oxygen was estimated through modelling efforts to be on the order of 25% of the total ion escape rates today (Lammer et al., 2006) and has yet to be determined with measurements. Nevertheless, the neutral escape at present rates from the Venusian atmosphere is not a significant source for the atmospheric evolution.

On the other hand, the non-thermal ion escape mechanisms are important at Venus. Due to the lack of an intrinsic magnetic field, the ionosphere of Venus interacts directly with the solar wind. The incoming EUV radiation ionizes the upper atmospheric particles, which, if exposed to the solar wind, may get “picked up” by the motional electric field and escape in the magnetosheath (Luhmann et al., 2004). Ions created inside the induced magnetosphere may instead be transported to the nightside by a pressure gradient (Knudsen et al., 1980). The ions can then be accelerated above the escape velocity of around 10 km/s by either the ambipolar electric field, forming from the separation of heavy ions and lighter electrons, or the draped magnetic field in the magnetotail (Hartle & Grebowsky, 1990; Barabash, Fedorov, et al., 2007; Dubinin et al., 2011; Collinson et al., 2016). A recent study by Masunaga et al. (2019) showed that less than 30% of oxygen ions escape through the pick-up process in the magnetosheath, while the rest escapes through the induced magnetotail.

The Pioneer Venus Orbiter (PVO) mission estimated the escape rates when it orbited Venus during 1978-1992 (Colin, 1980). From measurements during 1979 to 1986, the electron altitude profiles in the nightside was determined to have an average density of 39 cm^{-3}, which together with the estimated average ion velocity equivalent to 13 eV, gave an average escaping flux of $5{\cdot}10^{25}$ O^+/s, if the average was assumed for the entire disk of Venus (Brace et al., 1987). This number could be an overestimation, as Venus Express measurements later showed that the flux is mainly located in the central magnetotail and near the boundary region (Barabash, Fedorov et al., 2007). Therefore, the estimated escape rates from Brace et al. (1987) should likely be divided by at least a factor 5 (Fedorov et al., 2011). Using magnetometer measurements in the magnetotail during 1979 to 1984, and assuming a simple draping pattern of magnetic fields in the Venusian magnetotail, McComas et al. (1986) calculated the plasma density, velocity and temperature from the MHD momentum equation. The escape rate was estimated to $6{\cdot}10^{24}$ O^+/s. However, the time averaged magnetic field draping in the Venusian magnetotail may be more asymmetrical (Zhang et al., 2010) and the escape rate may be an underestimation. Ion flow measurements near the equatorial terminators showed that there was a significant flow of O^+ across the terminator, that is enough to sustain the nightside ionosphere of Venus (Knudsen et al., 1980). If assumed equal over the full disk of Venus it provides $5{\cdot}10^{26}$ O^+/s to the nightside that can potentially escape (Knudsen and Miller, 1992). The total flux is an upper limit, as the flow in the North Pole terminator region has a significant dawn-to-dusk component in the flow in addition to its trans-terminator component (Persson et al., 2019). Nevertheless, the main portion of the ions flowing trans-terminator does not lead to escape as Venus does have a significant nightside ionosphere composed of gravitationally bound ions (Knudsen and Miller, 1992).

Venus Express (VEx) measurements have shown that the total average escape rate from Venus today is $(3\text{-}6){\cdot}10^{24}$ O^+/s (see review by Futaana et al., 2017). The escape rates from VEx are thus lower than those found from the PVO measurements. This ambiguity may be explained by the difference in the upstream solar wind and solar parameters. From solar minimum to maximum, the O^+ escape rate tends to decrease slightly due to an increase in the Venusward fluxes in the near magnetotail, although the effect is strongest on the H^+ escape rate (Kollmann et al., 2016; Persson et al., 2018). On the other hand, during high dynamic pressure events the escape rates increase by a factor 1.9 (Edberg et al., 2011). In this study, we analyze the data from the full Venus Express mission during 2006-2014 to characterize the escape rate from the Venusian atmosphere with respect to the upstream parameters solar wind energy flux and solar EUV flux. We assume that the Venusian plasma environment respond systematically to the upstream conditions and can investigate the average state for each set of upstream parameters. The solar EUV flux was chosen since it is the main source of ion production. The increase in the EUV flux leads to an increase in the number of particles available in the ionosphere. The solar wind energy flux represents the amount of available energy in the solar wind and is directly related to the energy of the escaping particles. A part of the solar wind energy is transferred to the upper atmospheric particles which may lead to additional escape (Futaana et al. 2017). The purpose of this study is to find an empirical relation between the escape and these upstream parameters (section 3), which we then use for extrapolating the results backwards in time to calculate the total historical ion escape from the Venusian atmosphere (section 4).

2. Instrumentation and method

We use data from the Ion Mass Analyser (IMA), a part of the Analyser of Space Plasma and Energetic Atoms (ASPERA-4) instrument package on board Venus Express. IMA uses a top-hat electrostatic analyser to differentiate the energy of the incoming ions in the range 0.01-36 keV with the energy resolution $\Delta E/E=7\%$. The flying direction of the ion in the 360˚x90˚ (~2π sr) field-of-view is resolved by 16 azimuthal sectors of 22.5˚ each and elevation deflector plates scanning the elevation plane over 16 (5.6˚ wide) steps. Each full ion distribution is sampled over angle and energy every 192 s. The mass-per-charge is differentiated for M/Q=1-44 amu through an assembly of permanent magnets. The instrument is described in further detail by Barabash, Sauvaud et al. (2007).

All measurements of IMA obtained from April 2006 to November 2014 are used to calculate the escape rate to estimate the O^+ outflow. The mass is separated as described in Fedorov et al. (2011), where the heaviest species are assumed to be O^+. The average escape rates are calculated by the method developed in Persson et al. (2018) with improvements to achieve acceptable statistics with the separation for different upstream parameters as outlined below.

In order to formulate the escape flux as a function of the solar wind energy flux and the solar extreme ultraviolet (EUV) flux, we first need to estimate these parameters. The upstream solar wind moments are calculated from H^+ flux distributions measured by IMA outside the Venusian bow shock on VEx inbound and outbound orbit segments. Distributions for which the expected solar wind incident flow direction (corrected for aberration) is outside the instrument field-of-view, or blocked by spacecraft surfaces, are excluded. The valid solar wind H^+ distributions measured outside the bow shock are subsequently integrated moment-wise over solid angle and energy (for E >100 eV) to yield total solar wind H^+ densities and bulk velocities. Each O^+ measurement is then assigned the solar wind H^+ density and velocity that is closest in time within the same orbit period. As the full passage of the induced magnetosphere for Venus Express is short (around 2 hours) the expected deviation from the upstream solar wind at the exact time of O^+ measurement is small on a statistical basis.

Venus Express carried no dedicated instrument to monitor the solar EUV flux, instead we estimate it using Earth-based measurements. We used the Solar EUV Experiment (SEE) on the Thermosphere Ionosphere Mesosphere Energetics Dynamics (TIMED) spacecraft (Woods et al., 2005). The TIMED/SEE measurements are propagated to the nearest point in time that Venus would have observed the same solar disk, accounting for the Carrington rotation period, and scaled in intensity to the Venusian heliocentric distance. The daily-averaged EUV irradiance from the solar disk is quasistable on timescales of several days, limited by a rotational modulation of 20% at 17-22 nm and 10% at longer wavelengths. Therefore, the typical error incurred from this propagation is estimated to be typically less than ~7% (Thiemann et al., 2017; Ramstad et al., 2018). When the Earth-Venus separation was $|\Delta L_S|$ <45° the two planets are taken to have simultaneously observed roughly the same solar disk, as such we use TIMED/SEE observational (15 min) averages intensity-scaled to Venus without propagation in time (Ramstad et al., 2018). Here, we define the EUV flux as wavelengths within 1-118 nm and integrate over wavelength to find the total solar EUV flux. The frequency distribution of the derived EUV flux and solar wind energy flux at Venus at the time of each IMA measurement are shown in Figure 1. The data is divided into two EUV flux conditions: high and low EUV, separated at 0.007 Wm^{-2}, and five solar wind energy flux bins within each solar EUV condition.

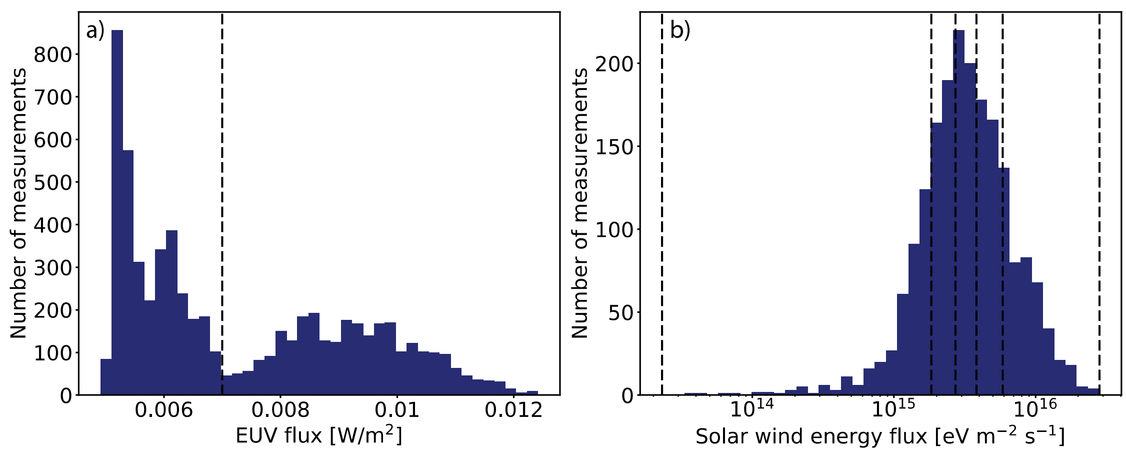

Figure 1. Frequency distributions of a) the solar EUV flux at Venus, propagated from 1 A.U, separated into high and low condition at 0.007 Wm^{-2} (dashed line), and b) the upstream solar wind energy flux calculated from the IMA measurements outside the bow shock of Venus, separated into five bins (dashed lines).

Average differential flux distributions are made from the O^+ measurements. Similar to Persson et al. (2018), the differential flux is organized by five degrees of freedom: two spatial dimensions (spacecraft position), two flying directions of the ions, and one for their energies. We used the Venus-Solar-Orbiter (VSO) cylindrical geometric frame to define the spatial bins. In the VSO frame, the X-axis points along the line from Venus to the Sun, and R is the distance from the X axis. The cylindrical geometric frame is valid if we assume an axisymmetric magnetotail, ignoring any effects of the asymmetry along the solar wind motional electric field, $E_{mot} = -v_{sw} \times B_{IMF}$, where v_{sw} is the solar wind velocity and B_{IMF} is the interplanetary magnetic field (McComas et al., 1986; Perez-de-Tejada, 2001; Jarvinen et al., 2013). As the sensitivity of the choice of frame for the escape rate calculations is small (Nordström et al., 2013), the assumption is deemed valid. The flying directions θ, φ of the ions are determined from the location of the VEx spacecraft at the time of the measurement, similar to Figure 1 in Ramstad et al. (2015). The elevation angle θ determines the radial velocity component, while the azimuth angle φ determines the velocity in the tangential-lateral plane.

Based on each upstream parameter, we separate the dataset of IMA O^+ observations into 10 groups. For each group, we produce maps of O^+ flux (Figure 2). Here, the magnetotail of Venus is divided into spatial bins with ΔX = ΔR = 0.3 Rv (Rv = Venus radii = 6052 km). The flux map $F_X(X_i, R_j)$ is obtained by integration of the 5-dimensional differential flux $\bar{J}(X_i, R_j, \varphi_k, \theta_l, \mathrm{E}_m)$ over the energy and angular dimensions.

$$F_x(X_i, R_j) = \int \bar{J}(X, R, \varphi, \theta, \mathrm{E}) \cos^2(\theta) \cos(\varphi) d\varphi d\theta\, dE$$

$$= \sum \bar{J}(X_i, R_j, \varphi_k, \theta_l, \mathrm{E}_m) \cos^2(\theta_l) \cos(\varphi_k) \Delta\varphi\Delta\theta\, \Delta E_m \; (1)$$

The energy width ΔE is computed so that the energy is divided as to be linearly distributed in velocity width with Δv = 5 km/s. The angular space is divided to have azimuth bin size of Δφ = 7.2˚ and elevation bin size of Δθ = 3.6˚. The average differential flux $\bar{J}(X_i, R_j, \varphi_k, \theta_l, \mathrm{E}_m)$ was calculated through an arithmetic mean of the measurements in each spatial bin for each upstream condition. Note that the differential flux $\bar{J}$, flying direction φ, θ and energy E are here corrected for the spacecraft velocity.

Figure 2 shows examples of the total fluxes in the X_{VSO} direction in each spatial grid for the ten chosen upstream conditions. In general, the fluxes are on average tailward (reddish bins), with a few bins with dominating Venusward flux (blueish bins). The Venusward flux is more prominent for the high solar EUV conditions, which agrees with the results that the return flows increase from solar minimum to solar maximum as reported in Persson et al. (2018). In addition, the number of bins with dominating Venusward fluxes decrease with increasing solar wind energy flux, specifically for the high EUV case. This is mainly due to an increase in energy of the O^+ out from the planet with increasing solar wind energy flux, where the Venusward fluxes does not change significantly over the changing solar wind energy flux conditions.

The net escape rate is then calculated from the flux $F_x(X_i, R_j)$ as

$$Q_{O^+} = \sum_i \frac{1}{N_i} \sum_j F_x(X_i, R_j) 2\pi R_j \Delta R,$$

where N_i is the number of slices used in the X direction, R_j is the radius of the center of the spatial bin used, and ΔR is the radial width of the spatial bin. The escape rates are calculated from the bins in the interval X = [-2.3, -1.4] R_V and R = [0, 1.2] R_V. The calculated net escape rates for each of the ten chosen upstream conditions is shown in Table 1.

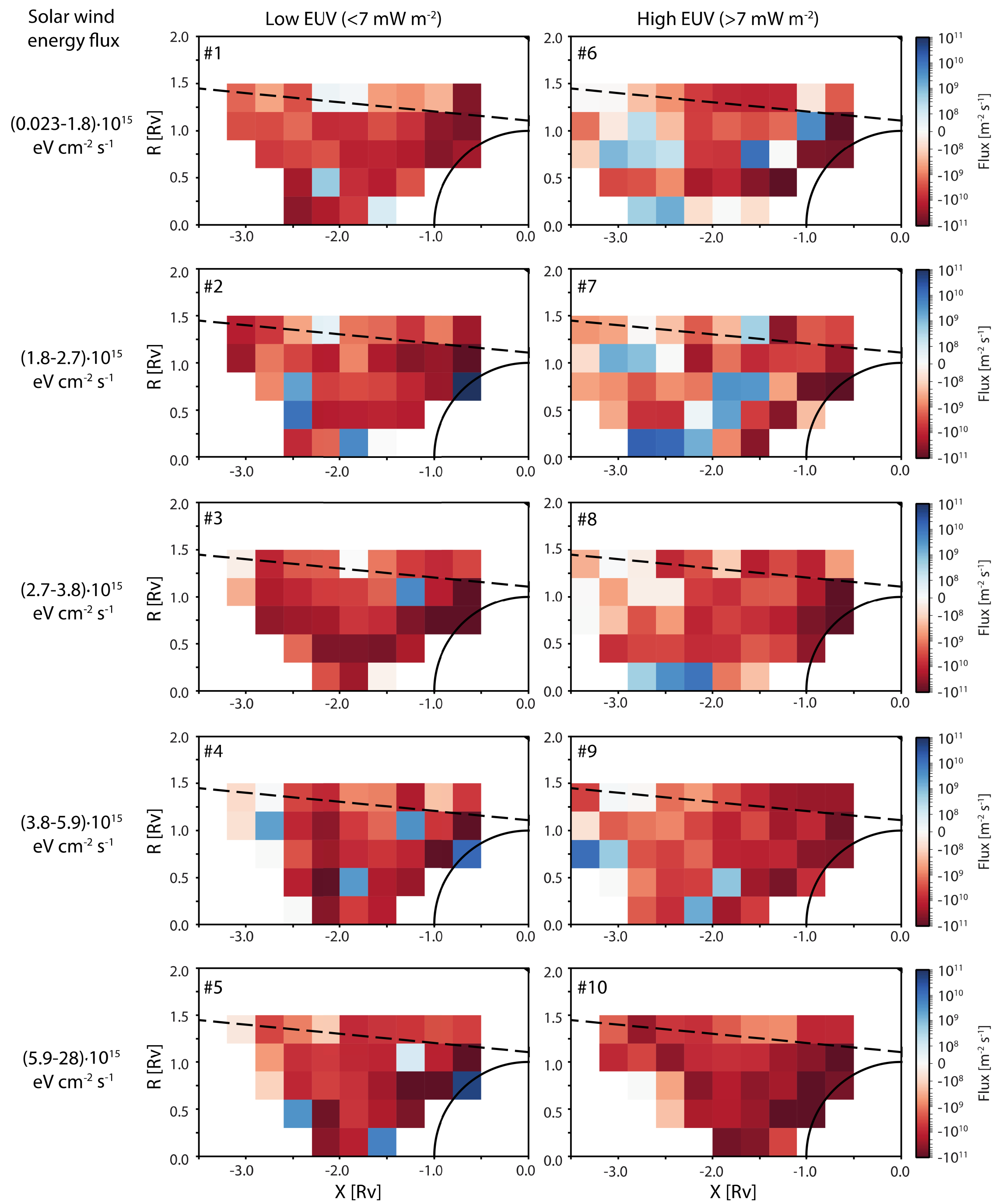

Figure 2. Maps of the O^+ flux in the Venusian plasma environment in cylindrical VSO coordinates, for each case of upstream parameters used in this study. The color depicts the flux in the X_{VSO} direction, where reddish bins represent tailward flux and blueish bins represent Venusward flux. The total escape rate calculated for each case #1-10 are tabulated in Table 1.

3. Upstream parameter dependence for the O^+ escape rate

Figure 3 shows the escape rates of O^+ from Venus through the magnetotail and the dependence the escape has on the solar wind energy flux and solar EUV radiation flux, which is also tabulated in Table

1. The average escape is ~2·10^{24} s^{-1}, which is close to the range of previous studies using VEx/IMA measurements at (3-6)·10^{24} s^{-1} (see review in Futaana et al., 2017). The dependence on the upstream parameters is fitted with a power function $Q_{O+} = Q_0 \cdot F^{\alpha}$ for the solar wind energy flux, for high and low solar EUV flux respectively, to investigate the strength of the dependences.

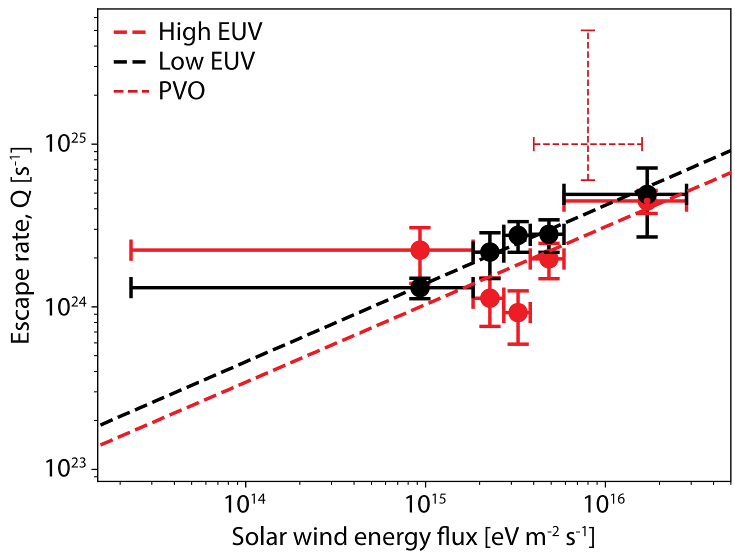

Figure 3. The escape rate for each of the five separated ranges of solar wind energy flux using high and low EUV flux. The vertical error bars show the standard error of the escaping flux and the horizontal error bars show the range for each upstream condition used to calculate the escape rates. The dashed lines present the best fit of a logarithmic function to the escape rate; $Q_{O+} = Q_0 \cdot F^{0.5\pm0.3}_{energy,SW}$, where $Q_0 = 7.1 \cdot 10^{16}$ for high EUV and $Q_0 = 8.5 \cdot 10^{16}$ for low EUV. The added red dashed cross shows the range of the escape rates determined from the PVO measurements (Brace et al., 1987; McComas et al., 1986), and the estimated average range of solar wind energy flux during the PVO era (McEnulty, 2012).

Table 1. Calculated average escape rates with standard errors for all upstream solar condition cases studied[a]

#	$F_{SW,energy}$ (10^{15} eV m^{-2} s^{-1})	I_{EUV} (mW m^{-2})	Q_{O+} (10^{24} s^{-1})
1	0.023-1.8	<7	1.3 ± 0.2
2	1.8-2.7	<7	2.2 ± 0.7
3	2.7-3.8	<7	2.8 ± 0.6
4	3.8-5.9	<7	2.8 ± 0.6
5	5.9-28	<7	4.9 ± 0.2
6	0.023-1.8	>7	2.2 ± 0.8
7	1.8-2.7	>7	1.1 ± 0.4

8	2.7-3.8	>7	0.9 ± 0.3
9	3.8-5.9	>7	2.0 ± 0.5
10	5.9-28	>7	4.5 ± 0.7
11[a]	4-16[b]	>7	6 - 50

[a] Case #11 is the estimated average PVO condition, plotted in Figure 3. [b]Estimated from McEnulty (2012).

From Figure 3, we clearly see that the O^+ escape rate increases with increasing solar wind energy flux, where the fitted logarithmic function to the high and low EUV conditions respectively gives the same relation $Q_{O+} \propto F_{energy,SW}^{0.5\pm0.3}$, where $Q_0 = 7.1 \cdot 10^{16}$ for high EUV and $Q_0 = 8.5 \cdot 10^{16}$ for low EUV. This indicate that the escape of planetary ions is dependent on the amount of available energy in the solar wind and that energy is transferred through the induced magnetosphere boundary to the atmospheric particles. To escape the planet, the planetary ions need to reach escape velocity (~10 km/s). With an increase in transferred energy from solar wind to atmospheric particles, more ions can reach above the escape velocity and escape the planet. Even with the clear dependence, the relation is quite weak, with a small increase in the escape rate as the solar wind energy flux increases. This is in agreement with previous discussions of the escape rates during solar minimum (Fedorov et al., 2011), solar minimum and maximum (Masunaga et al., 2019), and during high dynamic pressure events such as CMEs and CIRs which only increased the escape rates by a factor 1.9 (Edberg et al., 2011).

On the other hand, the results indicate that the escape rate only have a weak dependence on the solar EUV flux. The trend is the same for the low and high EUV conditions, where the escape rate is on average a factor <2 lower for the high solar EUV flux compared to the low solar EUV flux. As the EUV flux itself does not change more than a factor of 2 between the high and low cases, a weak dependence is not surprising. However, a decrease in escape rate with increasing solar EUV flux is opposite the general idea that an increase in production leads to increased material that can and will escape. This is explained by an increased fraction in the Venusward directed flow during the solar maximum, as stated previously (Persson et al., 2018; Masunaga et al., 2019). The trend of increased return flows is also clear in Figure 2, where the number of blueish bins, that indicate a major component towards Venus, is increased from low to high solar EUV flux. In addition, as the solar EUV flux is the main source for ion production, an increase in the EUV leads to an increase in the number of ions that can potentially escape the planet. Therefore, the results can also imply that all ions that are produced cannot escape through the magnetotail. Presumably, with more ions in the ionosphere, the energy available will be shared between more ions which may decrease the average velocity per ion. Even though there are more ions, there will be a smaller percentage above the escape velocity (~10 km/s) which may lead to an insignificant change in the total escape rate.

As the largest ion production is on the dayside, by solar EUV radiation ionisation, the ions need to be transported from the dayside to the nightside in order to escape down the magnetotail. This transport may be a limiting factor for the total escape rate. A large day-to-night flow of ions with ~5 km/s was measured in the equatorial terminator region (Knudsen et al., 1980). Assuming the same flow over the full disk of Venus, the flow accounts for a transport of up to $5 \cdot 10^{26}$ O^+/s from dayside to nightside (Knudsen and Miller, 1992). Though, the flow in the north pole terminator region was recently found to have a more complex behaviour, with a significant flow along the terminator (Persson et al., 2018). Taking into account that the flow is not uniform over the entire disk, the total flow from dayside to nightside is likely smaller than $5 \cdot 10^{26}$ O^+/s. In addition, a significant portion of the ions flowing into the nightside contributes to the nightside ionosphere (Knudsen and Miller, 1992). Even so, the flow is likely substantial enough to not limit the total escape rate from the Venusian atmosphere.

Escape rate results from the PVO mission are also included in Figure 3, ranging from $6 \cdot 10^{24}$ s^{-1} (McComas et al., 1986) to $5 \cdot 10^{25}$ s^{-1} (Brace et al., 1987). Although, the upper limit is likely overestimated by at least a factor 5 (Fedorov et al., 2011). The average solar wind energy flux was estimated from the solar wind velocity and density distributions from PVO measurements shown by McEnulty (2012). It is clear that the average solar wind energy flux was higher during the PVO era than the VEx era. In general, the escape rates from the PVO mission are consistent with the expected from our fitted logarithmic function within a factor of 2 difference (see Figure 3). In addition, the studies from the PVO era did not take into account that there is a significant return flow in the magnetotail, which decreases the total escape rates.

Measurements during extreme solar events, such as coronal mass ejections, show that the local O^+ flux at above escape velocity can increase as much as 100 times the nominal flux (Luhmann et al., 2007). It is important to take into account that it is challenging to get the full picture from only one measurement point, during such transient events, and estimate the increase in the total escape rate. Edberg et al. (2011) showed that, on average, the escape rate in the magnetotail region increases by a factor 1.9 during high dynamic pressure transient events. Indeed, our results agree, where from medium solar wind energy flux to high solar wind energy flux conditions, the escape rates increase by a factor 1.9 for the low EUV radiation case. The high EUV radiation flux case shows an even larger increase of a factor 3.8 from medium to high solar wind energy flux. The detailed physics of the escape rate will be investigated in a future study.

These results indicate that the ion escape process at Venus is energy-limited, i.e. the amount of energy input to the ionosphere is limiting the total escaping ion flux from the planet. Compare this to Mars, which was found to be source-limited, i.e. almost all ions supplied to the region energized by the solar wind gain sufficient energy to escape, and so the ion production rate limits the supply and thus the total escaping flux, rather than the amount of energy available (Ramstad et al., 2017). This may be explained by the fundamental difference in the size and gravity of Venus and Mars leading to an escape velocity twice as high on Venus (~10 km/s) compared to Mars (~5 km/s). The results can also be compared to results of ion escape from Earth. Schillings et al. (2019) investigated the influence of the solar dynamic pressure and solar EUV flux on the O^+ escape rates and found that the escape in the plasma mantle is positively correlated with the dynamic pressure, but there is a very small correlation with the solar EUV flux. A comparison between Earth and Venus is complex due to fundamental differences between the planets, which include, but are not limited to, the presence of an intrinsic magnetic field and the atmospheric composition (e.g. Gunell et al., 2018). However, the similar escape velocities (~10-11 km/s) and the similarity in the dependence on the upstream parameters, indicate that both Earth and Venus have an energy-limited escape, while the smaller Mars have a source-limited escape. Nevertheless, a direct comparison between the escape rates is challenging and we look forward to new advances in the field of planetary escape comparisons in future studies.

4. Total escape over 3.9 Ga

The logarithmic relations between the escape rate and the solar wind energy flux can be used to extrapolate the escape rates backwards in time. In order to make the extrapolation, information on the evolution of the solar wind is needed. The solar wind flux at the Venusian orbital distance can be calculated from the mass loss rate evolution of the Sun. From the absorption of the Lyman-α emission line measured for astrospheres of stars similar to the Sun, the mass loss rates are estimated and used to interpolate the solar mass loss rate back to ~3.9 Ga, $\dot{M} \propto t^{-2.33\pm0.55}$ (Wood, 2006). To extract the solar wind energy flux for the extrapolation, the evolution of the solar wind velocity is needed. From a MHD model of the solar wind, Airapetian and Usmanov (2016) estimated the solar wind speed at 0.7 Gyr, 2 Gyr and today (stars in Figure 4a). We used a logarithmic fit to interpolate between these solar wind speeds and estimate the evolution of the solar wind velocity over the past 3.9 Ga (Figure 4a). With the solar wind velocity and flux, the solar wind energy flux is calculated (Figure 4d), which provides the evolution of the atmospheric ion escape from Venus over the past 3.9 Gyrs (Figure 4e). Due to the weak relation between the solar wind energy flux and the escape rate, the escape rate only increases by about one order of magnitude to $Q_{O^+}(3.9\ Ga) = 3.2 \cdot 10^{25}$ s^{-1}, with a 1σ confidence interval of $[3.4 \cdot 10^{24}, 5.8 \cdot 10^{26}]$ s^{-1}.

As there is no clear trend on the EUV flux relation with the escape this relation has not been included in the extrapolation. However, earlier in the solar history the EUV flux was 100-1000 times stronger than it is today (Ribas et al., 2005). This would mean a significant increase in the local ion production in the Venusian dayside upper atmosphere and potentially a significant increase in the returning ion fluxes. The increase in solar flux would also heat up the atmosphere, causing an expansion of the thermosphere (e.g. Erkaev et al., 2013), and cause an increase in the neutral thermal escape of H, which would also create a drag force on O that can cause neutral oxygen escape. These are effects that we cannot infer from available measurements, instead substantial modelling is needed, and thus an elaborate discussion on the EUV flux effect on the escape rate is out of scope for this study.

Using the escape rate extrapolation from the solar wind energy flux relation, the total accumulated mass escaped from Venus through ion escape to space is estimated (Figure 4f). To account for the full O^+ ion escape, an escape through the magnetosheath is included as 30 % of the total escape (Masunaga et al., 2019). With the escape rate over the past 3.9 Ga the total mass that escaped to space as ions is calculated as $3.2 \cdot 10^{16}$ kg (1σ confidence interval: [$8.3 \cdot 10^{15}$, $2.7 \cdot 10^{17}$]), which accounts for ~0.007 % of the total current atmospheric mass of Venus of $4.8 \cdot 10^{20}$ kg, i.e. approximately 6 mbar of the equivalent surface pressure at Venus (out of 93 bar). In other words, the results in this study indicate that heavy ion escape to space has not had a strong influence on the evolution of the Venusian atmosphere.

Another important comparison to make is with the total amount of water present in the Venusian atmosphere. If we assume that all the O^+ escaping over the past 3.9 Ga originated from the water, which is likely since the escape rate ratio of H^+ and O^+ is 2, the stoichiometric ratio of water, (Barabash, Fedorov et al., 2007; Persson et al., 2018) we can calculate how much of that water could have escaped to space. This leads to a total mass of water lost from the atmosphere through non-thermal escape in the magnetotail aof $3.6 \cdot 10^{16}$ kg, or a global equivalent water layer of 0.3 m. Today the total water content in the atmosphere is $8 \cdot 10^{15}$ kg (Lecuyer et al., 2000), but the historical water content on Venus was presumably something between 1 % to more than 100% of Earth's current water inventory of $1.4 \cdot 10^{21}$ kg (see review in Kulikov et al., 2006). A water content of $1.4 \cdot 10^{21}$ kg corresponds to a global equivalent water depth of ~12 km. Therefore, the results indicate that the loss of oxygen, emanating from water, cannot be explained solely by escape to space. Some part of the oxygen could have ended up in the surface through oxidation of the surface materials (Albarède, 2009). However, the high pressure at the surface does not allow for a high diffusion of volatiles into the surface materials. Therefore, the diffusion of oxygen into the surface materials hardly account for the full loss of water content in the Venusian atmosphere (Gillmann and Tackley, 2014). To further understand the history of water in the Venusian atmosphere, the loss of hydrogen to space should be constrained, which due to the lighter mass is more challenging to determine, and is therefore left for a future study. The results of the oxygen escape do indicate that either water was not as abundant in the Venusian early history as previously assumed, or some piece of the understanding of the historical escape of atmospheric particles to space is still missing. A similar study at Mars indicates the same conclusions; the non-thermal escape of O^+ ions to space cannot account for the total loss of atmospheric content. An extrapolation of the current escape rates and its dependence on the upstream parameters lead to a total of up to ~10 mbar lost to space during the past 3.9 Ga (Ramstad et al., 2018).

It is important to mention that the escape rate extrapolation can constrain only the trends inferred from the current interaction between the solar wind and the Venusian upper atmosphere. The historical behavior of the atmospheric escape from Venus and the effects of the upstream parameters cannot be predicted through the current study alone. A future event study of the Venusian escape rates during an extreme space weather event, such as was done on Mars (Ramstad et al., 2017) and Earth (Schillings et al., 2018), would further constrain the escape rates for the upper part of the solar wind energy flux range. In addition, a sophisticated study including modelling efforts of both the effect of varying upstream parameters on the interaction with the Venusian induced magnetosphere, and the evolution of the Sun and its parameters, together with the results from current measurements to calibrate the numbers, would provide additional understanding of the evolution of the escape from the Venusian atmosphere.

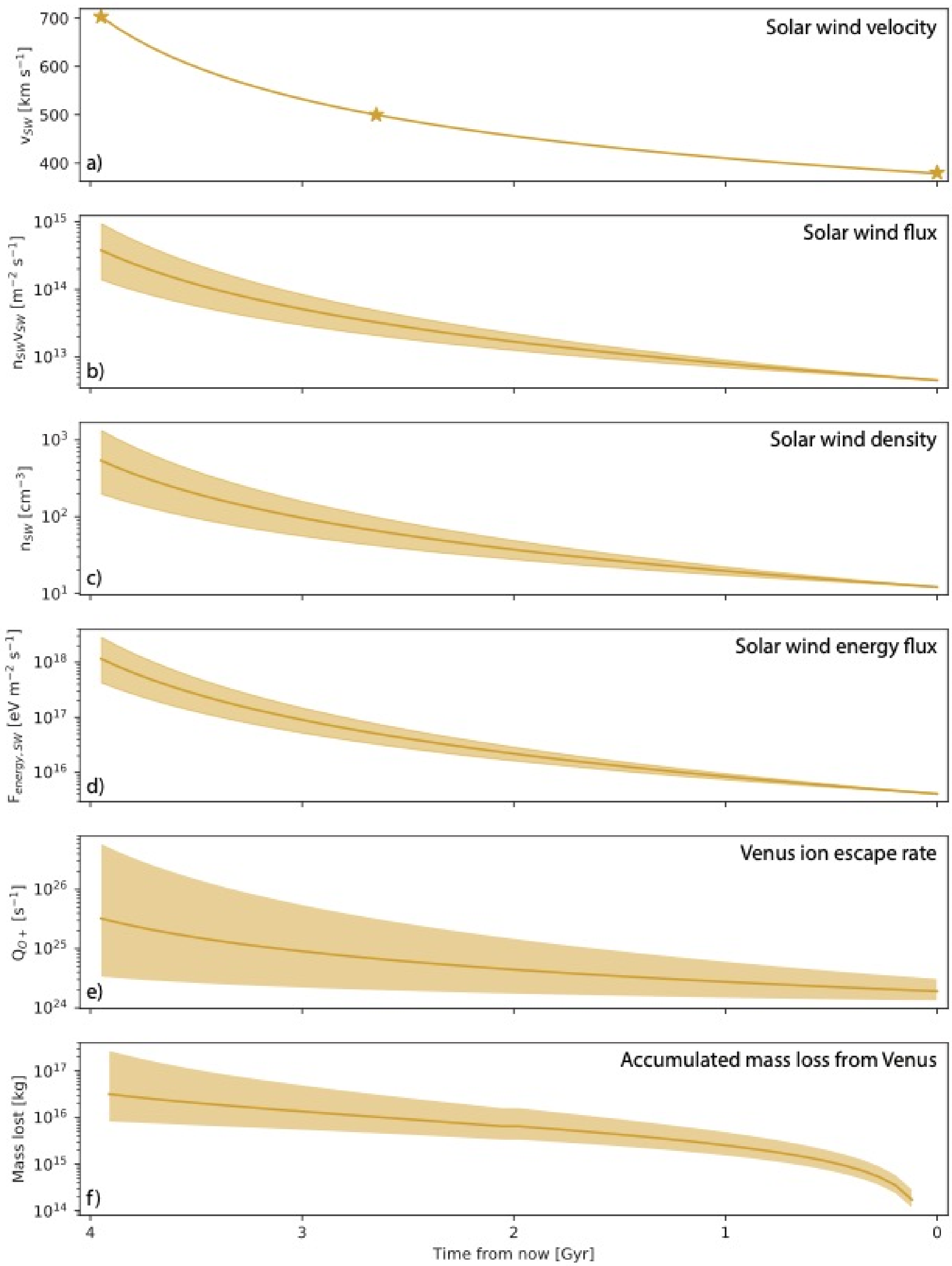

Figure 4. Evolution of upstream parameters over the past 4.6 Ga and the corresponding ion escape from Venus. a) solar wind velocity (where the stars represent the velocities reported in Airapetian and Usmanov, 2016), b) solar wind flux, c) solar wind density, d) solar wind energy flux, e) ion escape from Venus using the fitted dependence on solar wind energy flux, f) accumulated mass lost from Venus through ion escape over the past 4.6 Ga. The error on the solar wind parameters are

propagated from the error on the mass loss evolution of our Sun (Wood, 2006), and the error on the escape and mass loss are from both errors on upstream parameters and error on the fitted escape.

Conclusions

We have determined the current relation between the escape of O^+ through the magnetotail of Venus and the upstream solar wind and solar conditions. The escape is dependent on the solar wind energy flux as $Q_{O+} = Q_0 \cdot F_{energy,SW}^{0.5\pm0.3}$, where $Q_0 = 7.1 \cdot 10^{16}$ for high EUV and $Q_0 = 8.5 \cdot 10^{16}$ for low EUV. The solar EUV flux shifts the escape rate by a factor ~<2 from high solar EUV to low solar EUV. This shift mainly comes from an increased fraction of return flows from low to high solar EUV conditions.

Using the relation between the solar wind energy flux and O^+ escape rate, we extrapolated the escape rate backwards in time to 3.9 Ga, to characterize the total escape of O^+ from the Venusian atmosphere. The total escaping mass of O^+ is $3.2 \cdot 10^{16}$ kg. Assuming that all the O^+ originated from water, the total water escaped from the Venusian atmosphere over the past 3.9 Ga is $3.6 \cdot 10^{16}$ kg or equal to a 0.3 m water depth if spread equally over Venus. The escaping mass is higher than the total mass of water in the present Venusian atmosphere, but cannot account for a historical massive terrestrial-like ocean on the Venusian surface.

Acknowledgments

The Swedish contribution to the ASPERA-4 experiment on board Venus Express was supported by the Swedish National Space Agency (SNSA). We acknowledge the European Space Agency (ESA) for supporting the successful Venus Express mission. M. Persson acknowledges support to her graduate studies from SNSA (Dnr: 129/14). ASPERA-4/IMA data used in this study are publicly available via the ESA Planetary Science Archive at https://www.cosmos.esa.int/web/psa/venus-express.

References

Airapetian, V. S. and Usmanov, A. V. (2016). Reconstructing the solar wind from its early history to current epoch. The Astrophysical Journal Letters, 817(2):L24.

F. Albarède (2009). Volatile accretion history of the terrestrial planets and dynamic implications. Nature, 461:1227 – 1233.

Barabash, S., Fedorov, A., Sauvaud, J. J., Lundin, R., et al. (2007) The loss of ions from Venus through the plasma wakes. Nature, 450:650–653.

Barabash, S., Sauvaud, J.-A., Gunell, H., Andersson, H., Grigoriev, A., Brinkefeldt, K., et al. (2007). The analyser of space plasmas and energetic atoms (ASPERA-4) for the Venus Express mission. Planetary and Space Science, 55:1772–1792.

Brace, L. H., W. T. Kasprzak, H. A. Taylor, et al. (1987). The ionotail of Venus: Its configuration and evidence for ion escape. Journal of Geophysical Research, 92(A1):15–26.

Colin, L. (1980). The Pioneer Venus program. Journal of Geophysical Research: Space Physics, 85(A13):7575– 7598.

Collinson, G. A., Frahm, R. A., Glocer, A., Coates, A. J., et al. (2016). The electric wind of Venus: A global and persistent ”polar wind”-like ambipolar electric field sufficient for the direct escape of heavy ionospheric ions. Geophysical Research Letters, 43.

Donahue, T. M., Grinspoon, D. H., Hartle, R. E., and Hodges, Jr., R. R. (1997) Ion/neutral Escape of Hydrogen and Deuterium: Evolution of Water. In Bougher S. W., Hunten, D. M., and Phillips, R. J., editors, Venus II: Geology, Geophysics, Atmosphere, and Solar Wind Environment, page 385.

Dubinin, E., Fraenz, M., Fedorov, A., Lundin, R., Edberg, N., Duru, F., and Vaisberg, O. (2011). Ion energization and escape on Mars and Venus. Space Science Reviews, 162(1):173–211.

Edberg, N. J. T., Nilsson, H., Futaana, Y., Stenberg, G., Lester, M., Cowley, S. W. H. et al. (2011). Atmospheric erosion of Venus during stormy space weather. Journal of Geophysical Research: Space Physics, 116(A9), A09308.

Erkaev, N. V., Lammer, H., Odert, P., Kulikov, Y. N., Kislyakova, K. G., Khodachenko, M. L., et al. (2013). XUV-exposed, non-hydrostatic hydrogen-rich upper atmospheres of terrestrial planets. part I: Atmospheric expansion and thermal escape. Astrobiology, 13(11):1011–1029. PMID: 24251443.

Fedorov, A., Barabash, S., Sauvaud, J. A., et al. (2011). Measurements of the ion escape rates from Venus for solar minimum. Journal of Geophysical Research, 116:A07220.

Futaana, Y., Stenberg Wieser, G., Barabash, S., and Luhmann, J. G. (2017). Solar wind interaction and impact on the Venus atmosphere. Space Science Reviews, 212(3):1453–1509.

Gillmann, C. and Tackley. P. (2014). Atmosphere/mantle coupling and feedbacks on Venus. Journal of Geophysical Research: Planets, 119(6):1189–1217.

Gunell, H., Maggiolo, R., Nilsson, H., Stenberg Wieser, G., Slapak, R., Lindkvist, J., et al. (2018). Why an intrinsic magnetic field does not protect a planet against atmospheric escape. A&A, 614, L3 (2018) Doi: 10.1051/0004-6361/201832934

Hartle , R. E. and Grebowsky, J. M. (1990). Upward ion flow in ionospheric holes on Venus. Journal of Geophysical Research, 95(A1):31–37.

Ingersoll, A. P. (2969). The runaway greenhouse: A history of water on Venus. Journal of the Atmospheric Sciences, 26(6):1191–1198.

Jarvinen, R., Kallio, E., and Dyadechkin, S. (2013). Hemispheric asymmetries of the Venus plasma environment. Journal of Geophysical Research, 118:4551–4563.

Knudsen, W. C., Spenner, K., Miller, K. L., and Novak, V. (1980). Transport of ionospheric O+ ions across the Venus terminator and implications. Journal of Geophysical Research, 85(A13):7803–7810.

Knudsen, W. C. and Miller, K. L. (1992). The Venus transterminator ion flux at solar maximum. Journal of Geophysical Research: Space Physics, 97(A11):17165–17167.

Kollmann, P., Brandt, P., Collinson, G. A., et al. (2016). Properties of planetward ion flows in Venus' magnetotail. Icarus, 274:73–82.

Kulikov, Y., Lammer, H., Lichtenegger, H., Terada, N., Ribas, I., Kolb, C.et al. (2006). Atmospheric and water loss from early Venus. Planetary and Space Science, 54(13):1425 – 1444.

Lammer, H., Lichtenegger, H., Biernat, H., Erkaev, N., Arshukova, I., Kolb, C., et al. (2006). Loss of hydrogen and oxygen from the upper atmosphere of Venus. Planetary and Space Science, 54(13):1445 – 1456.

Lecuyer et al. (2000), Comparison of carbon, nitrogen and water budgets on Venus and the Earth, Earth and Planetary Science Letters, 33-40.

Luhmann, J. G., Ledvina, S. A., and Russell, C. T. (2004). Induced magnetospheres. Advances in Space Research, 33:1905–1912.

Luhmann, J. G., Kasprzak, W. T., and Russell, C. T. (2007). Space weather at Venus and its potential consequences for atmosphere evolution. Journal of Geophysical Research: Planets, 112(E4), E04S10.

Masunaga, K., Futaana, Y., Persson, M., Barabash, S., Zhang, T. Et al. (2019). Effects of the solar wind and the solar EUV flux on O+ escape rates from Venus. Icarus, 321:379 – 387.

McComas, D. J., H. E. Spence, C. T. Russell, and M. A. Saunders. (1986). The average magnetic field draping and consistent plasma properties of the Venus magnetotail. Journal of Geophysical Research: Space Physics, 91(A7):7939–7953.

McElroy, M. B., M. J. Prather, and J. M. Rodriguez. (1982). Loss of oxygen from Venus. Geophysical Research Letters, 9:649–651.

McEnulty, T. R. (2012). Oxygen Loss from Venus and the Influence of Extreme Solar Wind Conditions, (Doctoral dissertation). Retrieved from UC Berkeley Library, CA, US. (http://digitalassets.lib.berkeley.edu/etd/ucb/text/McEnulty_berkeley_0028E_13126.pdf). Location: UC Berkeley, CA, US.

Nordström, T., G. Stenberg, H. Nilsson, S. Barabash, and T. L. Zhang. (2013). Venus ion outflow estimates at solar minimum: Influence of reference frames and disturbed solar wind conditions. Journal of Geophysical Research: Space Physics, 118(6):3592–3601.

Pérez-de Tejada, H. (2001). Solar wind erosion of the Venus polar ionosphere. Journal of Geophysical Research: Space Physics, 106(A1):211–219.

Persson, M., Y. Futaana, A. Fedorov, H. Nilsson, M. Hamrin, and S. Barabash. (2018) H+/O+ escape rate ratio in the Venus magnetotail and its dependence on the solar cycle. Geophysical Research Letters, 45(20):10,805–10,811.

Persson, M., Y. Futaana, H. Nilsson, G. Stenberg Wieser, M. Hamrin, A. Fedorov, T. Zhang, and S. Barabash. (2019). Heavy ion flows in the upper ionosphere of the venusian north pole. Journal of Geo- physical Research: Space Physics.

Ramstad, R., S. Barabash, Y. Futaana, H. Nilsson, X.-D. Wang, and M. Holmström. (2015). The Martian atmospheric ion escape rate dependence on solar wind and solar EUV conditions: 1. seven years of Mars Express observations. Journal of Geophysical Research: Planets, 120:1298–1309.

Ramstad, R., S. Barabash, Y. Futaana, M. Yamauchi, H. Nilsson, and M. Holmström. (2017). Mars under primordial solar wind conditions: Mars express observations of the strongest CME detected at mars under solar cycle #24 and its impact on atmospheric ion escape. Geophysical Research Letters, 2017GL075446.

Ramstad, R., S. Barabash, Y. Futaana, H. Nilsson, and M. Holmström. (2017). Global mars-solar wind coupling and ion escape. Journal of Geophysical Research: Space Physics, 2017JA024306.

Ramstad, R., S. Barabash, Y. Futaana, H. Nilsson, and M. Holmström. (2018). Ion escape from mars through time: An extrapolation of atmospheric loss based on 10 years of mars express measurements. Journal of Geophysical Research: Planets, 123(11):3051–3060.

Ribas, I., E. F. Guinan, M. Gu¨del, and M. Audard. (2005) Evolution of the solar activity over time and effects on planetary atmospheres. i. high-energy irradiances (1-1700Å). The Astrophysical Journal, 622(1):680.

Schillings, A., Nilsson, H., Slapak, R., Wintoft, P., Yamauchi, M., Wik, M. et al. (2018). O^+ escape during the extreme space weather event of 4–10 September 2017. Space Weather, 16, 1363–1376. Doi: 10.1029/2018SW001881

Schillings, A., R. Slapak, H. Nilsson, M. Yamauchi, I. Dandouras, and L.-G. Westerberg. (2019). Earth atmospheric loss through the plasma mantle and its dependence on solar wind parameters. Earth, Planets and Space, 71(1):70.

Thiemann EMB, Eparvier FG, Woods TN. (2017). A time dependent relation between EUV solar flare light-curves from lines with differing formation temperatures. *J. Space Weather Space Clim.* **7**: A36.

Taylor, F. W., H. Svedhem, and J. W. Head. (2018). Venus: The atmosphere, climate, surface, interior and near-space environment of an earth-like planet. Space Science Reviews, 214(1):35.

Taylor, F. and D. Grinspoon. (2009) Climate evolution of Venus. Journal of Geophysical Research: Planets, 114(E9).

Wood, B. E. (2006). The solar wind and the sun in the past. Space Science Reviews, 126(1):3–14.

Woods, T. N., Eparvier, F. G., Bailey, S. M., Chamberlin, P. C., Lean, J., Rottman, G. J., Solomon, S. C., Tobiska, W. K., and Woodraska, D. L. (2005), Solar EUV Experiment (SEE): Mission overview and first results, *J. Geophys. Res.*, 110, A01312, doi:10.1029/2004JA010765.

Wordsworth, R. D. and Pierrehumbert, R. T. (2013). Water loss from terrestrial planets with CO2-rich atmospheres. The Astrophysical Journal, 778(2):154.

Zhang, T. L., W. Baumjohann, J. Du, R. Nakamura, R. Jarvinen, E. Kallio, A. M. Du, M. Balikhin, J. G. Luhmann, and C. T. Russell. (2010). Hemispheric asymmetry of the magnetic field wrapping pattern in the Venusian magnetotail. Geophysical Research Letters, 37(14), L14202.